Lazed and diffused: untangling noble gas thermochronometry data for exhumation rates

Matthew Fox[1] and David L. Shuster[2]

1. Department of Earth Sciences, University College London, London

2. Department of Earth and Planetary Science, University of California, Berkeley and Berkeley Geochronology Center, Berkeley

Abstract

Thermochronometric data can record the thermal history of rocks as they cool from high temperatures at depth to lower temperatures at the surface. This provides a unique perspective on the tectonic processes that form topography and the erosional processes that destroy it. However, quantitative interpretation of such data is challenging because multiple models can do an equally good job at reproducing the data. In this article, we describe how inverse modeling can be used to improve quantitative interpretations of noble gas thermochronometric data on a variety of scales ranging from mountain belts to individual mineral grains.

Introduction

Recent advances in our ability to infer the timings and rates of km-scale topographic changes using noble gas thermochronology have improved our understanding of geomorphic and tectonic processes. These datasets can quantify cooling associated with erosion in the geologic past, but require the use of models to help with the interpretation. *Forward* numerical models of how landscapes erode and rocks exhume have been used to understand the significance of thermochronometric data. In this sense, a set of parameters describing landscape evolution and tectonics are used to predict thermochronometric data. The focus of this article, in contrast, is to review applications of *inverse* models, which can be applied to noble gas thermochronometric data to determine thermal and exhumation histories. The goal is to highlight how these methods have been used to provide insight, and also some of their limitations.

Thermochronology methods are sensitive to the thermal histories of rocks over time intervals ranging from thousands of years to hundreds of millions of years, and are therefore useful for measuring rates of exhumation, which is the motion of rocks relative to Earth's surface. The well-known decay rates of radioactive nuclides, along with the temperature-dependent diffusion of daughter products, provide the basis of radiogenic nuclide thermochronology (Gautheron and Zeitler, this issue). For example, at relatively high temperatures (~400-300 ˚C), radiogenic ^{40}Ar produced by the decay of ^{40}K begins to be retained in micas. ^{40}Ar is retained in a range of crystallographic shapes and sizes (or sub-grain domains) that effectively have different temperature sensitivities, thereby constraining a continuous thermal history between 400 and 300 °C (Harrison and Lovera, 2014). At lower temperatures (~70 ˚C), radiogenic ^{4}He produced along the U and Th decay series begins to be retained in apatite crystals. Since the temperatures a rock experiences increases with depth, the temperature and time constraints provided by thermochronologic data can be converted to an exhumation rate history.

In order to resolve exhumation rate histories accurately, additional information is required. For example, multiple samples recovered from near to each other but from different elevations can, under the assumption of a relatively constant thermal structure of the crust, provide constraints on different durations of exhumation from the same depth with respect to sealevel (Wagner, Miller and Jager, 1979). This can be visualized by plotting an age-elevation relationship, with the slope of the line providing an estimate of the past exhumation rate (Figure 1). Alternatively, multiple ages from the same rock sample can be obtained using different thermochronometric systems (e.g. different mineral or decay schemes) sensitive to different temperatures, thereby constraining exhumation rates from different depths.

Here we highlight the importance and limitations of different inverse methods designed to extract information from thermochronometric data. We begin by describing methods that have been used to extract time-temperature information from thermochronometric data with a focus on *Thermal-History Models*. In many cases, however, exhumation rates are required for geological interpretations and therefore, we highlight work that has attempted to infer exhumation rates across mountain belts from thermochronometric data using *Thermokinematic Models*, and some of the associated complications with these approaches. In the last section, we take a closer look at inverse modeling developments applied to data treatment across single crystals. In particular, we highlight how combining laser ablation data with diffusion models of helium from individual crystals of apatite represents an important advance.

Thermal-History Models

A thermochronometric date doesn't necessarily reflect a single event; instead, it reflects the integrated thermal history experienced by the sample. The goal of thermal-history modeling is to recover time-temperature information from dates and other thermochronometry data. In many cases, recovering time-temperature information from thermochronometric data is a highly non-linear problem, in that a small change in model parameters can lead to a large change in model predictions. For example, consider a case where a rock is exhumed to the surface rapidly at 100 Ma and is then buried until it is re-exhumed very recently. If the model parameter describing temperature during this burial phase is increased from 0 ˚C to 30 ˚C there will be no significant change in the predicted apatite (U-Th)/He age. This is because the apatite (U-Th)/He system is not sensitive to these very low temperatures. However, as the temperature during burial continues to increase there will, at some stage, be rapid changes in model predicted apatite (U-Th)/He ages due to the non-linear dependence of He diffusivity on temperature. It is this non-linear temperature sensitivity that makes thermochronometry possible, but this also leads to challenges in data interpretation.

To extract information from this non-linear problem, *non-linear* inverse methods are used. Typically these are based on generation of many random time-temperature paths. Non-linear methods often require solving the forward model many, many times, which can be very expensive computationally. In contrast, linear inverse methods are based on computationally efficient matrix inversions, but often require making limiting simplifications - we will return to these types of methods later. For non-linear methods, random time-temperature paths can be used in a range of mathematical models to predict a range of data, such as fission track ages and length distributions (Ketcham et al. 2007), or noble gas-based thermochronometric ages and diffusion data. The models have the ability to characterize the changing efficiency of noble gas diffusion as crystal defects, and in particular radiation damage, accrue and anneal in the lattice structure of minerals (Flowers et al. 2009; Gautheron et al., 2009). The models can also account for samples comprising a range of crystallographic shapes and sizes (Harrison and Lovera, 2014; McDannell and Flowers, this issue). In order to describe a time-temperature path, some sort of parameterization is required, and for this discussion we will use a very simple parameterization in which a series of time-temperature points are linked by straight lines. The locations of the time-temperature points are our model parameters. These parameters are said to occupy the "parameter space"; we aim to explore this space, but must avoid getting lost in the process.

Thousands of candidate time-temperature paths are typically generated to find the best parameters (time-temperature points) describing time-temperature paths that predict the thermochronometric data. If paths are generated purely randomly, there is a good chance that the inversion algorithm will spend a large amount of time exploring time-temperature paths that do a poor job of predicting the observed thermochronometric data. One technique commonly used to speed up the search process is to use some form of prior knowledge, such as independent geologic constraints. For example, the formation age of the rock can be used as an indication of when to start the time-temperature paths in geological time, such that parameters older than this do not need to be tested. Another example is to force paths through a surface temperature condition at a time when there is a geologically constrained unconformity, meaning that high temperatures don't need to be tested during this time period.

A second technique used is to guide the search based on what has previously been successful. If a time-temperature path does a very good job at reproducing the data, then a new path can be generated that is very similar to this promising path. Part of the parameter space that produces a small misfit between the observed and predicted data is referred to as a minimum and mapping out these minima is a goal of inversions. However, if all the paths that are generated are too similar, the algorithm may become trapped in a local minimum. It is therefore important that a search-based algorithm has the ability to explore parameter space to find a global minimum, without getting trapped in a local minimum. These techniques–random versus guided searches of parameter space–have advantages and disadvantages, however both approaches have been shown to provide similar results.

The two most commonly used pieces of software designed to extract thermal history information from single samples using these two different approaches are HeFTy (Ketcham, 2005) and QTQt (Gallagher, 2012). HeFTy uses a purely random path generation procedure that can be guided by user-defined constraint boxes. This means that a time-temperature path is generated that must pass through these areas of parameter space. The ability of the path to predict the thermochronometric data is defined by asking whether it passes a statistical hypothesis using a goodness-of-fit test based on a "p-value". The purely random model has the benefit that it explores a range of model parameters. QTQt uses a reversible jump Markov Chain Monte Carlo algorithm to generate paths that are similar to the best models. By exploring parameter space around promising models, the algorithm can converge to a solution more quickly. In addition, QTQt's algorithm provides a means to choose how many time-temperature points are required based on the quality of the data.

As mentioned earlier, in order to gain more robust time-temperature information, additional thermochronometric data are required, either from different systems or different elevations. QTQt has the capability to model samples from different elevations within a vertical transect. In this case a thermal model is required to link the data. The thermal model employed by QTQt is a simple geothermal gradient that does not account for heat transport, but does provide the link between samples. In Figure 2, we highlight how incorporating additional data helps constrain different, but overlapping, portions of the same thermal history. In some cases, however, a more sophisticated thermal model is used that accounts for the effects of topography on the thermal structure of the crust, or the physics of heat flow. In the next section we describe some of the recent developments in approaches to using thermochronometric data to learn about geodynamic processes such as *exhumation rates*.

Geodynamics from Thermokinematic Models

Thermokinematic models provide a framework to use thermochronometric data not just to extract thermal histories but to directly constrain geodynamics by linking thermal histories to physical processes. Thermokinematic models used to interpret thermochronometry data have evolved, both as the questions asked of the data have evolved and as weaknesses in existing models have been identified. For example, the potential problem of topography leading to incorrect interpretations of age-elevation relationships (e.g., Manktlelow and Grasemann,1994) has been embraced, and thermochronometry is now used to measure evolving topography (e.g., House et al. 1998). Today, thermokinematic models solve the heat transfer equation based on user-defined kinematics and account for complex initial conditions, transient advection of heat, fluid flow and tectonic and geomorphic processes (Braun et al. 2012). In this way, a specific rock in a model can be tracked through time along its user-defined *kinematic* path to the surface. The temperature experienced along that path is recorded, and the resulting time-temperature path can be used to predict thermochronometric data. These thermokinematic models can be coupled to a non-linear inversion algorithm to find a best set of model parameters. Unlike in thermal-history models, where the model parameters are typically temperature-time points, model parameters in thermokinematic models may define the slip rate on a fault, the timings of topographic change or the thermal properties of rocks. The finite element code Pecube (Braun et al. 2012) is the most commonly used thermokinematic model. It uses state-of-the-art age models to predict thermochronometric data and guide a non-linear algorithm.

A compelling example of thermokinematic modelling using Pecube comes from Michael et al. (2018), who investigated the impact of Pleistocene glaciation on exhumation rates across the Olympic Mountains (Washington State, USA). Here exhumation is driven by accretionary processes as the Juan de Fuca plate subducts beneath the North American plate, resulting in predictable kinematics that can be approximated with an elliptical-shaped spatial pattern of exhumation rates that decrease from the center of the ellipse outwards. This ellipse is designed to approximate the spatial patterns of crustal accretion and rock uplift within a critically tapered orogenic wedge (Brandon et al., 1998). In this scenario, exhumation rates would increase towards the center of the ellipse. This pattern can be incorporated into a 3D thermo-kinematic model (Pecube: Braun et al. 2012) and used to predict the observed apatite (U-Th)/He and zircon (U-Th)/He data from the Olympic Mountains. By finding predicted data that match observed data, the location and size of the ellipse and the gradient in exhumation rates within the ellipse can be determined. In addition, temporal changes in exhumation rate can be parameterized and resolved. Michael et al. (2018) found that the data can be explained by an ellipse-shaped exhumation pattern which increases from ~0.25 km/Ma at the edge of the ellipse to 0.9 km/Ma at its center. In addition, they showed that Pliocene-Pleistocene alpine glaciations in the Olympic Mountains likely led to a 50-150% increase in exhumation rates in the past 2-3 Ma. This study highlights that if the underlying kinematics of exhumation can be inferred and parameterized, the parameters defining the ellipse and changes in rates through time can be explored. In some cases, however, this is not possible because the underlying kinematics of exhumation cannot be parameterized with a simple elliptical geometry. This may be because exhumation varies over a large area, it may be overly complex and computationally expensive, or the underlying spatial pattern of exhumation is unknown.

When the underlying exhumation function cannot be parameterized with less than about 20 model parameters, linear inverse methods are often required (Fox et al., 2014). In this approach a simple thermokinematic model is used to estimate the closure isotherm for each age in a dataset accounting for transient geotherms, perturbation of isotherms by topography, and thermochronometer and cooling-rate dependent closure temperatures (Dodson, 1973). For each age in the dataset, the distance to the closure isotherm can be written as the integral of the exhumation rate between today and the thermochronometric age. This integral formulation can be written as a linear system of equations that can be efficiently rearranged to find the unknown exhumation rate parameters. Samples are linked in space so that samples close together share the same exhumation rate history, and this linking enables the ages to resolve temporal changes in rate. This is because ages are forced to share similar exhumation rate histories with different ages constraining overlapping portions of time. One disadvantage of spatially linking samples in this way is that spatial and temporal patterns in exhumation rates might be smeared out, for example, across faults or other boundaries that have disparate exhumation rate histories (Fox et al. 2014; Schildgen et al. 2018)

Thermal-history and thermokinematic models have been used to test all sorts of geodynamic and geomorphic hypotheses, but measuring small amounts of recent erosion remains a challenge. In turn, key hypotheses, such as whether Pliocene-Pleistocene alpine glaciation can lead to enhanced erosion rates (e.g., Herman et al. 2013; Willenbring and Jerolmack, 2016; Michael et al., 2018, Schildgen et al. 2018), remain debated. In the next section, we describe $^{4}He/^{3}He$ thermochronometry in apatite, how it allows us to constrain this crucial shallow exhumation history, and how recent numerical modeling developments allow these grain-scale datasets help provide better resolved, quantitative thermal history information.

Grain-scale Inverse Models

Inverse models can also use grain-scale data to improve interpretation of themrochronometric data. To highlight a recent example where this has been done, we focus on two aspects of inverse modeling applied to ^{4}He/^{3}He datasets. In ^{4}He/^{3}He thermochronometry, a crystal is sequentially heated and the gas released during each heating step is measured isotopically using a noble gas mass spectrometer (Shuster and Farley, 2004). Because the gas is extracted by diffusion, during the first degassing steps gas is released primarily from the outermost parts of the apatite crystal. The next heating step releases gas from slightly deeper parts of the crystal and so on, until all the gas is released. To improve the quality of the data and obtain sample-specific diffusion data, two isotopes of helium are measured: ^{4}He, the naturally-occurring daughter product of radioactive decay, and ^{3}He, which is produced via nuclear reactions caused by proton irradiation of the sample prior to analysis. The ^{4}He signal contains information about the thermal history of the sample that must be extracted using inverse methods, but also the spatial distribution of the parent isotopes. The ^{3}He signal is spatially uniform and contains information about diffusion kinetics.

^{4}He/^{3}He data can be visualized on a ratio evolution diagram, where the cumulative fraction of ^{3}He released (ΣF^{3}He) is plotted on the x-axis, and the ^{4}He/^{3}He ratio of each step normalized by the bulk ^{4}He/^{3}He ratio (R_{step}/R_{bulk}) is plotted on the y-axis. We can predict what ^{4}He/^{3}He values are permissible in a ratio evolution diagram based on what we know about the spatial distribution of ^{4}He in an 'ideal' apatite crystal (i.e., close to spherical and with an uniform composition) for any given thermal history. However, we sometimes observe values that are outside of this permissible range (e.g., Figure 4a). The cause of unexpected results may be due to several factors: the analyzed crystals may be poorly approximated as spheres; the spatial distribution of ^{4}He may be strongly influenced by variations in parent isotope concentration within the crystal (e.g. chemical zoning); intra-crystal radiation damage may lead to spatial variations in the diffusion kinetics within the analyzed crystal (Ault and Flowers, 2012). This last factor would lead to zones throughout the crystal, that are more retentive of helium due to radiation damage, holding on to their helium until the final degassing steps.

Fox et al. (2014) explored different sources of unexpected diffusion behaviour using a very unusual result from the Appalachian Mountains. In this geologic setting, the exhumation rates have been slow for the last 200 million years, allowing radiation damage to accumulate. The importance of chemical zonation on the (U-Th)/He system had been previously established for these samples by looking at the effect of abrading the crystals (McKeon et al. 2014). Abrading effectively removed the outer portion of the crystal that had a different uranium and thorium concentration (or effective uranium, [eU] = [U]+0.24[Th], which accounts for the relative alpha particle productivity of U and Th; *Gastil et al.,* 1967; *Flowers et al.*, 2009) to the central part of the crystal. The ages obtained from these abraded crystals were used to extract a thermal history, whereas the ages from the un-abraded crystals remained unexplainable. By using ^{4}He/^{3}He thermochronometry, the ^{4}He being released from different parts of the crystal can be observed directly without the need for abrasion (Fox et al. 2014). During the first steps, the ratio of ^{4}He to ^{3}He is much lower than the bulk ratio (Figure 4). These low values persist until almost half the total amount of ^{3}He is released telling us that almost half of the crystal had released its gas. Then the ratio of ^{4}He to ^{3}He dramatically increases to almost three times the bulk ratio.

This indicates that almost all of the ^4He is coming from a relatively small, central portion of the crystal.

The next step was to quantify the spatial distribution of the ^4He-producing uranium and thorium using laser ablation inductively coupled plasma mass spectrometry (LA-ICPMS). In this method, a laser spot with a diameter of about 20 microns is fired at a polished section of the apatite crystal, which ablates small volumes of the crystal into a mass spectrometer (Farley et al. 2011). This highlighted that there was indeed a zone within the central part of the crystal with a higher [eU]. Therefore, a 3D model of the crystal was built accounting for spatial variability in ^4He production and intra-crystal radiation damage. Fox et al. (2014) found that both of these factors are required to explain the observed $^4He/^3He$ data (Figure 4). These data have prompted the development of efficient 3D crystal models and corresponding inverse methods, which are now suitable to tackle other geological problems and help resolve recent cooling of a sample to low-temperatures.

In a related study, Fox et al. (2017) found that even with the LA-ICPMS maps and 3D crystal models, $^4He/^3He$ datasets of apatites from Yosemite Valley were impossible to explain using thermal history modeling that accounted for these complexities. This is because the crystals were releasing too much ^4He during the initial degassing steps suggesting that zonation effects were important. It was only when the resolution of the elemental maps used to quantify zonation were improved, that thermal-history models were able to predict the data. It was possible to improve the resolution of these elemental maps using linear inverse methods by exploiting the fact that laser ablation spots overlap and thus the same spatial location on a crystal section will be sampled by multiple spots. In this scenario, multiple spots that measure the same part of the crystal may have different concentration values, smoothing zonation information (Ganguly et al., 1988). Deconvolving this information and finding an elemental map that has single values at each location and still gives the average values measured by the spots, increases the resolution of the map. In fact, the resolution depends on the degree to which the spots overlap, not their size (Figure 4B). Here, overlapping spots with diameters of 20 microns have been used to resolve concentrations over a narrow zone only ~5 microns wide. In turn, this inverse method is able to resolve finer-scale differences in parent isotope concentrations than is possible by simply interpolating between the measured values at the centers of the spots (e.g., Farley et al., 2011) and does not require the use of analytical instruments that are capable of operating with smaller spot sizes. Some degree of smoothing and blurring does occur, as shown by the comparison with the true zonation imposed to produce the synthetic data (Figure 4B), but this can be further minimized by collecting more overlapping spots. This is an example of where inverse methods have been applied to extract more information from a single crystal that can then be incorporated into thermal-history and thermokinematic models to infer geodynmic processes across entire mountain ranges.

Summary

Analytical and numerical modeling methods in noble gas thermochronology have complemented one another, enabling geoscientists to tackle geological problems from fresh perspectives. On the one hand, new analytical methods have been developed, and numerical methods have had to catch up to interpret these new datasets. On the other hand, numerical methods have opened up possibilities that have led to new types of datasets being developed. These exciting new developments will continue to push our understanding of Earth's dynamic surface.

Acknowledgements

We would like to thank Sam Johnstone and Kendra Murray for very helpful revisions and Emily Cooperdock, Marrissa Tremblay and Peter Zietler for handling the manuscript. MF is supported by NERC (NE/N015479/1).

Figure Captions

Figure 1. A) Cartoon showing the thermal structure below topography and the paths that rocks take from the depth. Topography perturbs the thermal structure of the crust, and the samples from the deepest parts of the valley may be sensitive to the evolution of topography. In this cartoon, the exhumation is controlled by surface processes and spatially variable rock uplift rates reflecting regional tilting and normal faulting on the left of the scene. B) The cooling histories of two samples from close together, but different elevations, are almost parallel (black curves). As a first order approximation, apatite fission track (AFT) and and apatite (U-Th)/He (AHe) ages record the time since a rock cooled below ~110^{o}C and 70^{o}C respectively. Because elevation differences can be related to temperature differences, different samples constrain cooling over slightly different time intervals. C) The simplest model used to link ages in terms of exhumation rate is a linear age-elevation relationship (AER). This model assumes that the closure isotherms are flat and stationary, and the model parameters are exhumation rate and closure depth that correspond, respectively, to the slope of the AER and the intercept. This model requires that samples are linked in space, and choices about how to link samples influence the inferred exhumation rate(s). In reality, the relationship between age and elevation may be non-linear due to the advection of heat, perturbation of isotherms by topography, topographic change, changes in exhumation rate, and many other factors.

Figure 2. Demonstration of how incorporating more data improves inverse model resolution. In A) and B), two ages are interpreted with a simple model that randomly generates time-temperature paths that fit the data, as shown by the red lines. All the paths go through a point constrained by the closure temperature and age. However, the red lines are not necessarily similar to the true cooling history shown by the black line. Here we imagine that panel A) is an apatite (U-Th)/He (AHe) age and B) is an apatite fission track (AFT) age. Combining the two ages requires making the assumption that the analyzed crystals share the same thermal history, and leads to increased resolution (C). Incorporating a low elevation sample constrains part of the same history, but this sample has traveled a shorter distance from the closure depth and the age is consequently younger (D). If a thermal model, even a simple thermal model of a uniform geothermal gradient, is used to link the samples, the younger age from the low-elevation sample helps constrain the recent cooling of the higher-elevation sample (E). In particular, paths are

forced to cool earlier so that the lower-elevation sample cools below its closure temperature. In order to link more samples and further improve resolution, a thermokinematic model is required that accounts for more complexities (F).

Figure 3. A) Topographic map of the Olympic Peninsula (Washington State, USA) highlighting the major river valleys (Elwha, Hoh, Queets, Quinault) that drain the mountains. The extent of the Cordilleran Ice Sheet and the moraines of major glaciers are shown in pink and the Hurricane Ridge fault is shown as the black dashed line. The changing geomorphic processes between glacial and interglacial periods led to temporal changes in exhumation rate, but the overall tectonics associated with accretion are assumed to be uniform. B) The exhumation pattern used for the study can be parameterized by changing the shape of the ellipse or the magnitude of the exhumation rate in the center of the ellipse. This approximates accretionary processes and the exhumation paths of rocks within the accretionary wedge (after Michael et al., 2018).

Figure 4. A) In order to explain complex apatite $^4He/^3He$ data from a sample in the Appalachian Mountains, a model was developed that accounted for measured effective uranium concentrations by LA-ICPMS (Fox et al. 2014). It was only by accounting for spatial variations in radiation damage (Flowers et al. 2009) and ^4He that the overall shape of the $^4He/^3He$ data could be predicted. This model used the time-temperature path recovered by McKeon et al. (2014). B) Example LA-ICPMS map of effective uranium (eU), constructed using a linear inverse method (Fox et al. 2017). The synthetic data were made using a zoned model with the 'true' widths of the zones shown on the left. The data are plotted as very small dots and are coloured based on the measured values. The measured areas are shown by the large overlapping spots. For example, the large white spot is the average of multiple zones, but the large black spot is completely within the green zone. The overlapping laser ablation spots povide redundant information that can be exploited to infer sub-spot size spatial resolution. Some smearing is expected but this can be reduced by collecting more data (Fox et al. 2017). This improved resolution is required to interpret some apatite $^4He/^3He$ data.

References

Ault, A.K. and Flowers, R.M., 2012. Is apatite U–Th zonation information necessary for accurate interpretation of apatite (U–Th)/He thermochronometry data? *Geochimica et Cosmochimica Acta*, *79*, pp.60-78.

Brandon, M.T., Roden-Tice, M.K. and Garver, J.I., 1998. Late Cenozoic exhumation of the Cascadia accretionary wedge in the Olympic Mountains, northwest Washington State. *Geological Society of America Bulletin*, *110*(8), pp.985-1009.

Braun, J., Van Der Beek, P., Valla, P., Robert, X., Herman, F., Glotzbach, C., ... & Prigent, C. (2012). Quantifying rates of landscape evolution and tectonic processes by thermochronology and numerical modeling of crustal heat transport using PECUBE. *Tectonophysics*, *524*, 1-28.

Dodson, M.H., 1973. Closure temperature in cooling geochronological and petrological systems. *Contributions to Mineralogy and Petrology*, *40*(3), pp.259-274.

Farley, K. A., Shuster, D. L., & Ketcham, R. A. (2011). U and Th zonation in apatite observed by laser ablation ICPMS, and implications for the (U–Th)/He system. *Geochimica et Cosmochimica Acta*, *75*(16), 4515-4530.

Flowers, R. M., Ketcham, R. A., Shuster, D. L., & Farley, K. A. (2009). Apatite (U–Th)/He thermochronometry using a radiation damage accumulation and annealing model. *Geochimica et Cosmochimica acta*, *73*(8), 2347-2365.

Fox, M., McKeon, R. E., & Shuster, D. L. (2014). Incorporating 3-D parent nuclide zonation for apatite 4He/3He thermochronometry: An example from the Appalachian M ountains. *Geochemistry, Geophysics, Geosystems*, *15*(11), 4217-4229.

Fox, M., Tripathy-Lang, A., & Shuster, D. L. (2017). Improved spatial resolution of elemental maps through inversion of LA-ICP-MS data. *Chemical Geology*, *467*, 30-41.

Fox, M., Herman, F., Willett, S. D., & May, D. A. (2014). A linear inversion method to infer exhumation rates in space and time from thermochronometric data. *Earth Surface Dynamics*, *2*(1), 47-65.

Gallagher, K. (2012). Transdimensional inverse thermal history modeling for quantitative thermochronology. *Journal of Geophysical Research: Solid Earth*, *117*(B2).

Ganguly, J., Bhattacharya, R.N. and Chakraborty, S., 1988. Convolution effect in the determination of composition profiles and diffusion coefficients by microprobe step scans. *American Mineralogist*, *73*(7-8), pp.901-909.

Gastil, R. G., Delisle, M. and Morgan, J., 1967. Some Effects of Progressive Metamorphism on Zircons. *Geological Society of America Bulletin*, *78*, p.879.

Gautheron, C., Tassan-Got, L., Barbarand, J. and Pagel, M., 2009. Effect of alpha-damage annealing on apatite (U–Th)/He thermochronology. *Chemical Geology*, *266*(3-4), pp.157-170.

Gautheron and Zeitler (2020), this issue

Harrison, T. M., & Lovera, O. M. (2014). The multi-diffusion domain model: past, present and future. *Geological Society, London, Special Publications*, *378*(1), 91-106.

Herman, F., Seward, D., Valla, P. G., Carter, A., Kohn, B., Willett, S. D., & Ehlers, T. A. (2013). Worldwide acceleration of mountain erosion under a cooling climate. *Nature*, *504*(7480), 423-426.

Herman, F., & King, G. E. (2018). Luminescence thermochronometry: Investigating the link between mountain erosion, tectonics and climate. *Elements*, *14*(1), 33-38.

House, M. A., Wernicke, B. P., & Farley, K. A. (1998). Dating topography of the Sierra Nevada, California, using apatite (U–Th)/He ages. *Nature*, *396*(6706), 66-69.

Ketcham, R. A. (2005). Forward and inverse modeling of low-temperature thermochronometry data. *Reviews in mineralogy and geochemistry*, *58*(1), 275-314.

Ketcham, R. A., Carter, A., Donelick, R. A., Barbarand, J., & Hurford, A. J. (2007). Improved modeling of fission-track annealing in apatite. *American Mineralogist*, *92*(5-6), 799-810.

Mancktelow, N. S., & Grasemann, B. (1997). Time-dependent effects of heat advection and topography on cooling histories during erosion. *Tectonophysics*, *270*(3-4), 167-195.

McKeon, R. E., Zeitler, P. K., Pazzaglia, F. J., Idleman, B. D., & Enkelmann, E. (2014). Decay of an old orogen: Inferences about Appalachian landscape evolution from low-temperature thermochronology. *Bulletin*, *126*(1-2), 31-46.

Michel, L., Ehlers, T. A., Glotzbach, C., Adams, B. A., & Stübner, K. (2018). Tectonic and glacial contributions to focused exhumation in the Olympic Mountains, Washington, USA. *Geology*, *46*(6), 491-494.

Reiners, P. W., & Brandon, M. T. (2006). Using thermochronology to understand orogenic erosion. *Annu. Rev. Earth Planet. Sci.*, *34*, 419-466.

Schildgen, T. F., van der Beek, P. A., Sinclair, H. D., & Thiede, R. C. (2018). Spatial correlation bias in late-Cenozoic erosion histories derived from thermochronology. *Nature*, *559*(7712), 89-93.

Shuster, D. L., & Farley, K. A. (2004). 4He/3He thermochronometry. *Earth and Planetary Science Letters*, *217*(1-2), 1-17.

Wagner, G. A., Miller, D. S., & Jäger, E. (1979). Fission track ages on apatite of Bergell rocks from central Alps and Bergell boulders in Oligocene sediments. *Earth and Planetary Science Letters*, *45*(2), 355-360.

Willenbring, J. K., & Jerolmack, D. J. (2016). The null hypothesis: globally steady rates of erosion, weathering fluxes and shelf sediment accumulation during Late Cenozoic mountain uplift and glaciation. *Terra Nova*, *28*(1), 11-18.

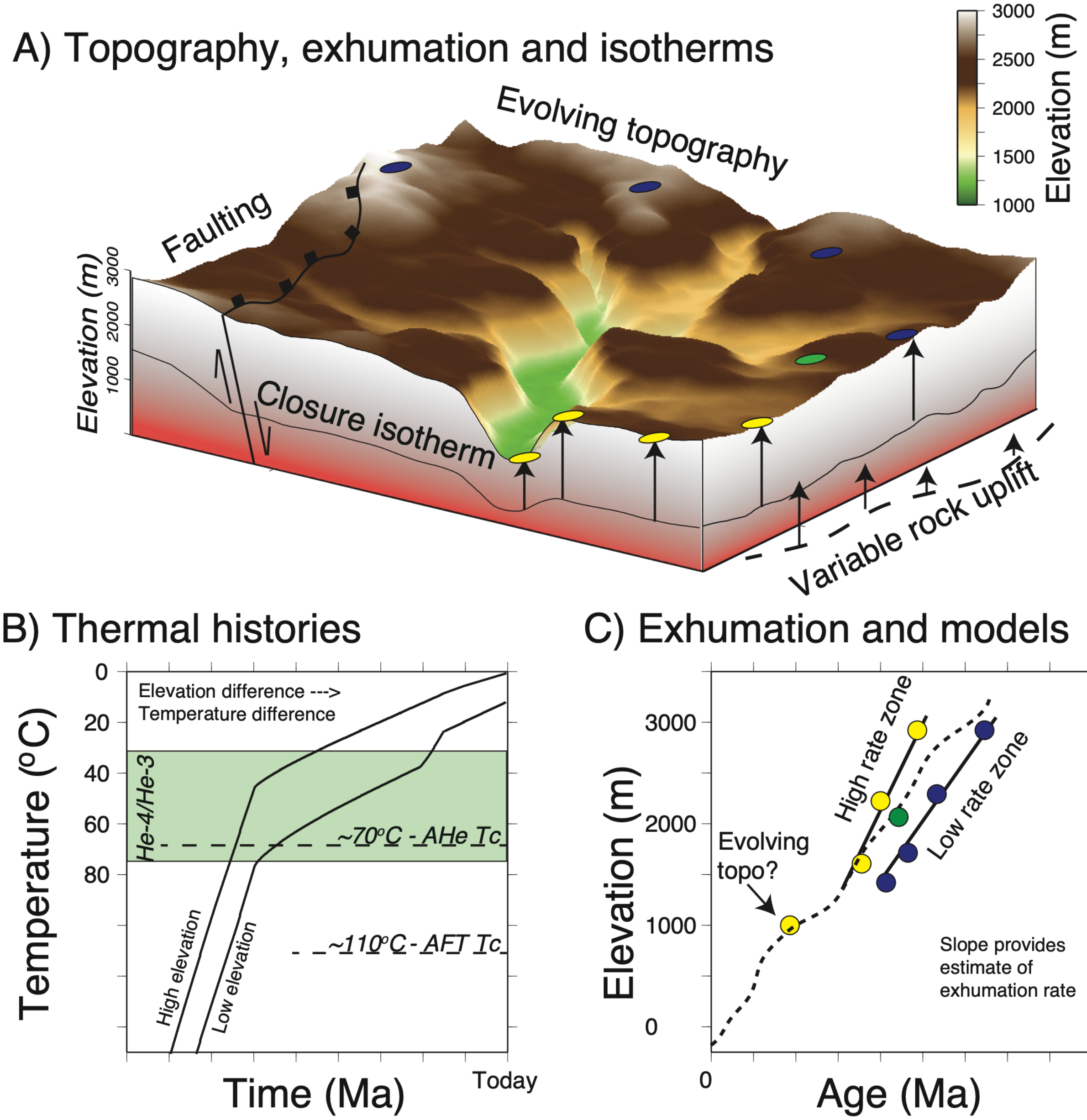

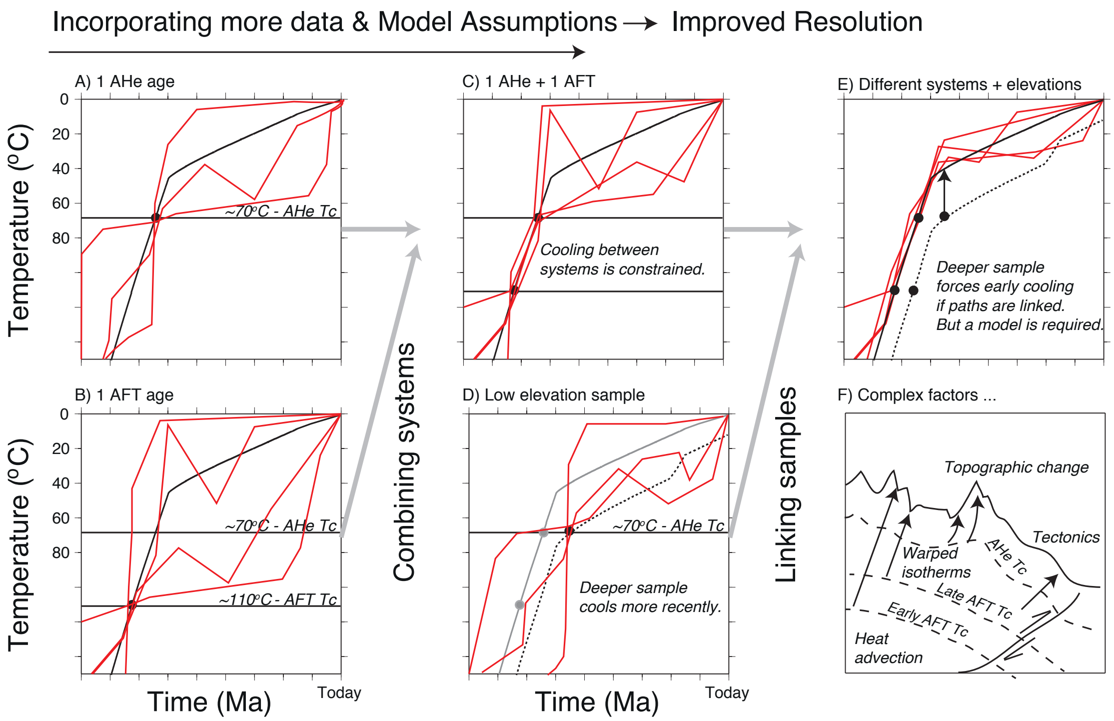

Incorporating more data & Model Assumptions → Improved Resolution
A) 1 AHe age
B) 1 AFT age
C) 1 AHe + 1 AFT
D) Low elevation sample
E) Different systems + elevations
F) Complex factors ...
Temperature (°C)
0
20
40
60
80
~70°C - AHe Tc
~110°C - AFT Tc
Cooling between systems is constrained.
Deeper sample cools more recently.
Deeper sample forces early cooling if paths are linked. But a model is required.
Combining systems
Linking samples
Time (Ma)
Today
Topographic change
Tectonics
Warped isotherms
AHe Tc
Late AFT Tc
Early AFT Tc
Heat advection

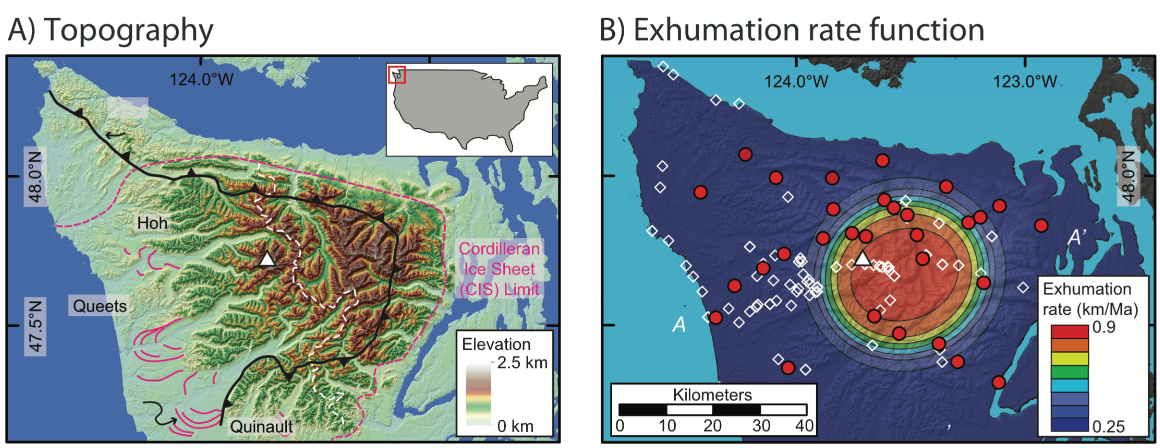

A) Topography
124.0°W
48.0°N
47.5°N
Hoh
Queets
Quinault
Cordilleran Ice Sheet (CIS) Limit
Elevation
2.5 km
0 km
B) Exhumation rate function
124.0°W
123.0°W
48.0°N
A
A'
Exhumation rate (km/Ma)
0.9
0.25
Kilometers
0
10
20
30
40

A) Elemental maps and diffusion

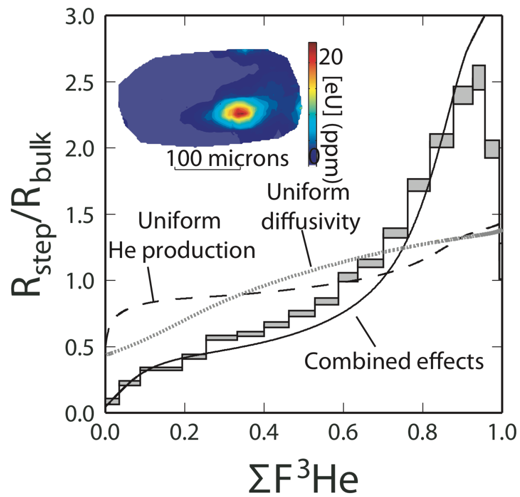

B) Inverse methods for LA-ICPMS